



Supplement of

Aerosol–cloud interactions studied with the chemistry-climate model EMAC

D. Y. Chang et al.

Correspondence to: D. Y. Chang (dongyeong.chang@mpic.de)

Table S1. Hygroscopicity of aerosol components characterized by the number of ions the salt dissociates into in water (μ), osmotic coefficient (ϕ), mass fraction of soluble material (ϵ), density (ρ_a) and molecular weight (M_a) of aerosol.

Component (j)	μ_j	ϕ_j	ϵ_j	ρ_j	M_j	B_j	κ_j
Ammonium sulfate	3.0	0.7	1.0	1.77	132.17	0.51	0.61
Sea salt	2.0	1.0	1.0	2.17	58.44	1.16	1.28
Soil dust	2.0	0.45	0.13	2.65	40.08	0.14	0.03
Organic carbon	1.0	1.0	0.047	2.0	12.11	0.14	0.1
Black carbon	1.0	1.0	1.7e-07	2.0	12.11	0.5e-7	0.0

For the multi-compound bulk aerosols (i.e., DU, BC, and OC) empirical parameters or estimations based on experiments are applied to the calculation of B_j ; the osmotic coefficient (ϕ_{DU}) is based on east Asian dust observed by Nishikawa et al. (1991) and Nishikawa (1993). To simplify the calculation of water uptake, the fixed parameters of ϕ_j and B_j are applied, which could be varied depending on the solution. The density (ρ_{DU}) and molecular weight (M_{DU}) of soil dust are based on the chemical composition of $CaSO_4$ in the aerosol submodel GMXe.

1.1 Taylor Diagram

Taylor diagrams based on Taylor (2001, 2005) summarizes the resemblance between two patterns (e.g., simulations and observation) with statistical values (i.e., the centered root mean squared (RMS) difference, the spatial pattern correlation, and the standard deviation). A Taylor diagram can be described with the following formula (Taylor, 2001):

$$E'^2 = \sigma_x^2 + \sigma_r^2 - 2\sigma_x\sigma_r R, \quad (1)$$

where R is the correlation coefficient, E' is the centered RMS difference between the model results and the observations (or reference data), and σ_x and σ_r are the standard deviations of the model results and the observations (or reference data), are given by;

$$R = \frac{\frac{1}{N} \sum_{n=1}^N (x_n - \bar{x})(r_n - \bar{r})}{\sigma_x \sigma_r} \quad (2)$$

$$E'^2 = \frac{1}{N} \sum_{n=1}^N [(x_n - \bar{x}) - (r_n - \bar{r})]^2 \quad (3)$$

$$\sigma_x^2 = \frac{1}{N} \sum_{n=1}^N [(x_n - \bar{x})]^2, \quad \sigma_r^2 = \frac{1}{N} \sum_{n=1}^N [(r_n - \bar{r})]^2 \quad (4)$$

To plot different variables (i.e., the relevant cloud and climate parameters) on the same diagram, the simulated standard deviation and centered RMS error are normalized by the corresponding observed standard deviation (σ_r). Note that the correlation coefficient (R) is not changed by a normalization. The normalized statistical variables are calculated with the following equation;

$$\hat{E}' = \frac{E'}{\sigma_r}, \hat{\sigma}_x = \frac{\sigma_x}{\sigma_r}, \hat{\sigma}_r = 1 \quad (5)$$

1.2 Skill score

To evaluate the performance of the EMAC model, a relative skill score is calculated with by the following formula (Taylor, 2001)

$$S = \frac{4(1 + R)}{(\hat{\sigma}_x + \frac{1}{\hat{\sigma}_x})^2(1 + R_0)}, \quad (6)$$

where R_0 is the maximum correlation coefficient (0.9976) in this study. This model skill score is determined by the pattern variability and correlation with observations. If the simulated standard deviation is close to the observed standard deviation (i.e., $\hat{\sigma}_x$ approaches 1) and the correlation coefficient increases (i.e., R is close to R_0), the model skill score (S) approaches 1 (most skillful). Note that the RMS error may not necessarily contribute to a high skill score. Further detailed information can be found in Taylor (2001).

Table S2. Continental and marine means and corresponding statistic variables (i.e., the standard deviation (σ)*, spatial pattern correlation coefficient (R), centered root mean square (E')* difference) used in the spatial pattern comparisons (Fig. ??) between the model simulations and observations, and their skill scores (S) (Table ??**).

	Continental					Marine				
TCC (-)	Mean	σ	R	E'	S	Mean	σ	R	E'	S
1-RH-REF	0.532	0.204	0.903	0.088	0.9513	0.715	0.158	0.865	0.079	0.9205
2-ST-REF	0.482	0.195	0.855	0.105	0.9287	0.539	0.198	0.789	0.122	0.7975
3-RH-STN	0.548	0.200	0.898	0.090	0.9497	0.722	0.154	0.868	0.077	0.9263
4-ST-STN	0.533	0.219	0.900	0.095	0.9401	0.618	0.169	0.786	0.105	0.8625
5-RH-HYB	0.539	0.202	0.903	0.090	0.9518	0.717	0.157	0.863	0.077	0.9207
6-ST-HYB	0.493	0.195	0.876	0.095	0.9392	0.563	0.191	0.817	0.105	0.8281
Obs. (MODIS)	0.520	0.196				0.7155	0.140			
SCRE (W/m^2)	Mean	σ	R	E'	S	Mean	σ	R	E'	S
1-RH-REF	-35.76	24.36	0.897	11.03	0.9025	-64.79	20.59	0.761	13.51	0.8599
2-ST-REF	-24.36	14.68	0.854	10.27	0.8592	-37.18	19.24	0.764	12.74	0.8761
3-RH-STN	-45.40	30.76	0.906	15.51	0.7778	-76.74	22.94	0.736	15.54	0.8106
4-ST-STN	-43.36	30.76	0.863	17.08	0.7603	-55.51	22.26	0.741	14.99	0.8248
5-RH-HYB	-38.23	25.38	0.909	15.51	0.8901	-68.99	21.90	0.762	15.54	0.8410
6-ST-HYB	-27.63	16.54	0.867	17.08	0.9111	-43.29	21.59	0.768	14.99	0.8481
Obs. (CERES)	-33.00	19.42				-52.84	17.59			
LCRE (W/m^2)	Mean	σ	R	E'	S	Mean	σ	R	E'	S
1-RH-REF	26.07	11.63	0.894	5.336	0.9479	29.48	13.24	0.868	6.595	0.9005
2-ST-REF	24.98	13.07	0.892	5.912	0.9319	23.97	11.87	0.826	6.777	0.9074
3-RH-STN	24.77	9.876	0.811	6.752	0.8858	30.19	13.19	0.864	6.655	0.8998
4-ST-STN	22.51	9.243	0.839	6.275	0.8778	26.66	11.89	0.865	5.989	0.9266
5-RH-HYB	25.96	11.11	0.881	6.752	0.9405	29.59	13.12	0.868	6.655	0.9032
6-ST-HYB	25.02	12.87	0.899	6.275	0.9391	24.62	11.88	0.830	5.989	0.9091
Obs. (CERES)	24.17	11.51				27.09	10.89			
Ptot (mm/day)	Mean	σ	R	E'	S	Mean	σ	R	E'	S
1-RH-REF	2.142	1.975	0.827	1.135	0.9117	3.348	2.665	0.833	1.529	0.7950
2-ST-REF	2.788	3.000	0.844	1.741	0.7434	3.039	2.394	0.825	1.361	0.8477
3-RH-STN	1.752	1.419	0.803	1.115	0.8378	3.441	2.681	0.814	1.600	0.7834
4-ST-STN	1.998	1.792	0.892	0.855	0.9453	3.321	2.516	0.8409	1.394	0.8304
5-RH-HYB	2.067	1.840	0.829	1.115	0.9155	3.366	2.656	0.830	1.600	0.7957
6-ST-HYB	2.720	2.876	0.863	0.855	0.7783	3.074	2.372	0.8279	1.394	0.8530
Obs. (GPCP)	2.118	1.868				2.904	1.817			
AOD (-)	Mean	σ	R	E'	S	Mean	σ	R	E'	S
1-RH-REF	0.217	0.167	0.784	0.108	0.8906	0.203	0.084	0.692	0.062	0.8219
2-ST-REF	0.202	0.156	0.817	0.095	0.9094	0.184	0.076	0.704	0.057	0.8489
3-RH-STN	0.236	0.174	0.759	0.117	0.8729	0.233	0.099	0.655	0.075	0.7429
4-ST-STN	0.227	0.179	0.803	0.108	0.8893	0.219	0.094	0.767	0.060	0.8183
5-RH-HYB	0.214	0.164	0.729	0.117	0.8646	0.215	0.087	0.635	0.075	0.7846
6-ST-HYB	0.200	0.155	0.769	0.108	0.8852	0.194	0.076	0.658	0.060	0.8260
Obs. (MODIS)	0.219	0.159				0.132	0.071			

*The normalized standard deviation ($\hat{\sigma}_x = \frac{\sigma_x}{\sigma_r}$) and CRMS difference ($\hat{E}' = \frac{E'}{\sigma_r}$) by the corresponding observed standard deviation (σ_r) are used in the Taylor diagrams (??). **Rating in Table ?? is based on skill

score (S), with following ranges ; 5 (1.000–0.9500); 4 (0.9499–0.9000); 3 (0.8999–0.8500); 2 (0.8499–0.7500); 1 (0.7499–0.6000); 0 (under 0.6000)

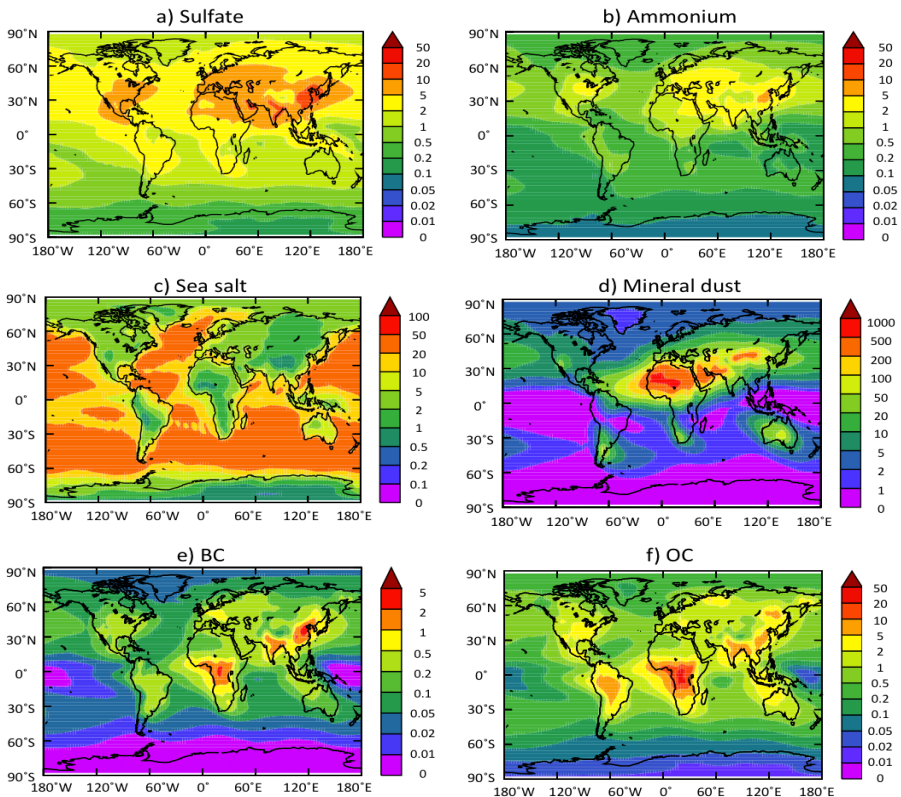


Fig. S1. Global distributions of the annual mean total aerosol column burden;(a) sulfate, (b) ammonium, (c) sea salt, (d) mineral dust, (e) BC, and (f) OC for ST-HYB, unit (mg/m^2).

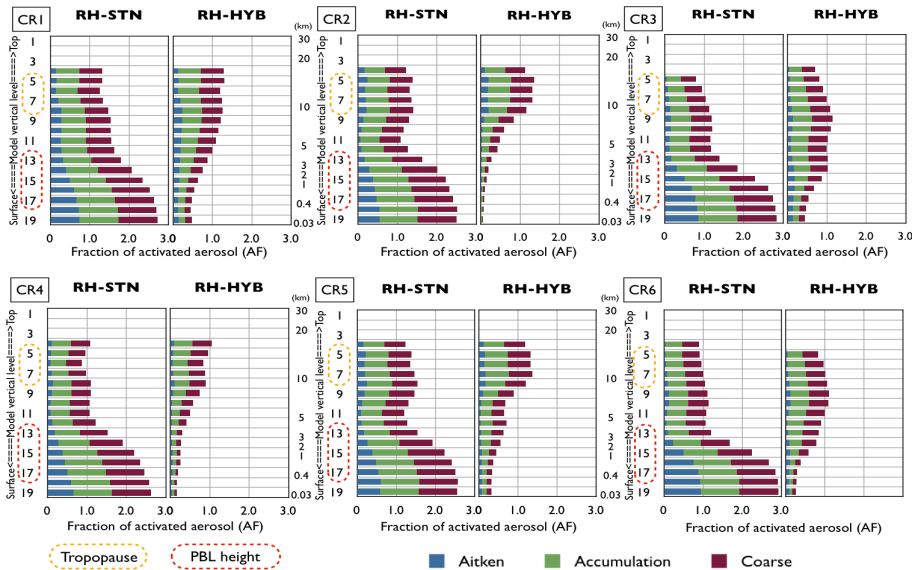


Fig. S2. Vertical distributions of the activated aerosol fraction in the selected continental regions (from CR1 to CR6) for RH-STN and RH-HYB.

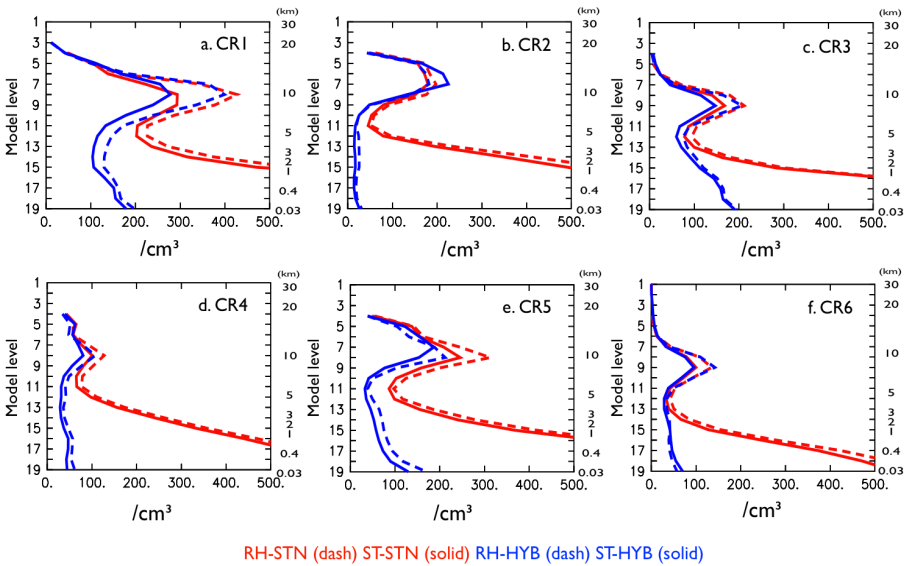


Fig. S3. Vertical distributions of activated aerosol (CCN) number concentration in the selected continental regions (CR) for RH-STN, ST-STN, RH-HYB, and ST-HYB.

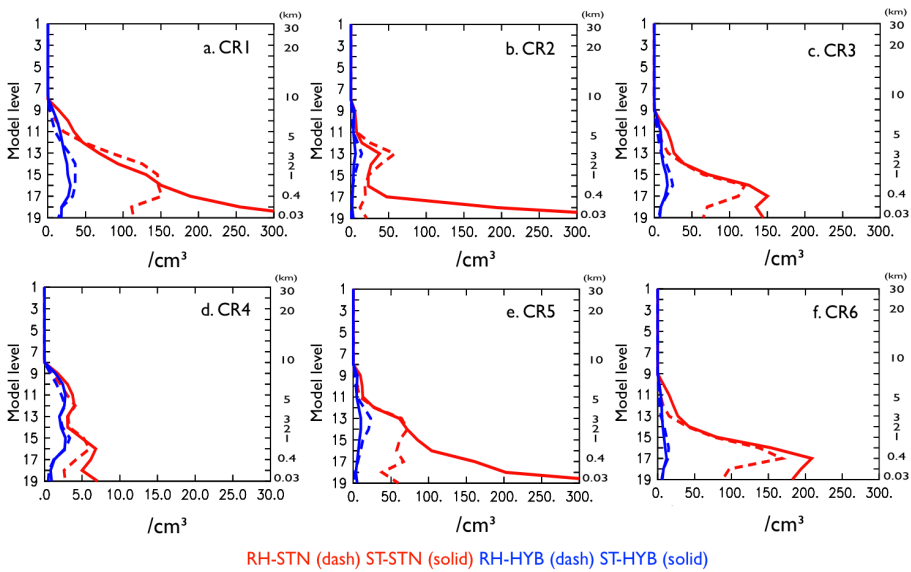


Fig. S4. Vertical distributions of cloud droplet number concentration (CDNC) in the selected continental regions (CR) for RH-STN, ST-STN, RH-HYB, and ST-HYB.

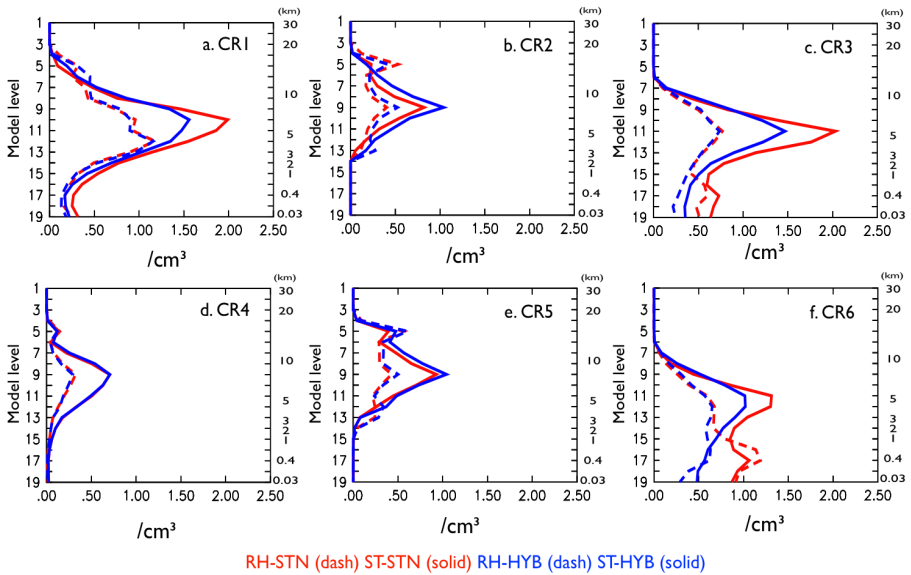


Fig. S5. Vertical distributions of ice crystal number concentration (ICNC) in the selected continental regions (CR) for RH-STN, ST-STN, RH-HYB, and ST-HYB.

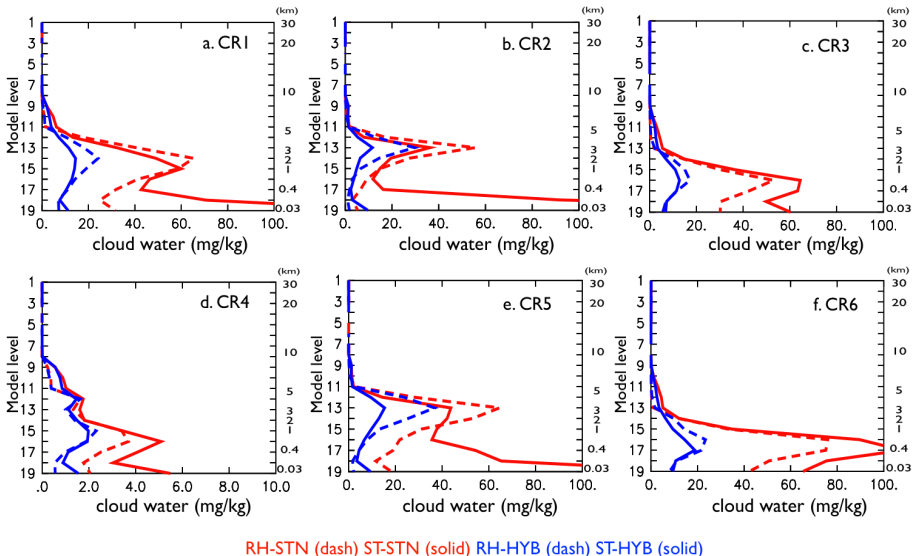


Fig. S6. Vertical distributions of cloud liquid water in the selected continental regions (CR) for RH-STN, ST-STN, RH-HYB, and ST-HYB.

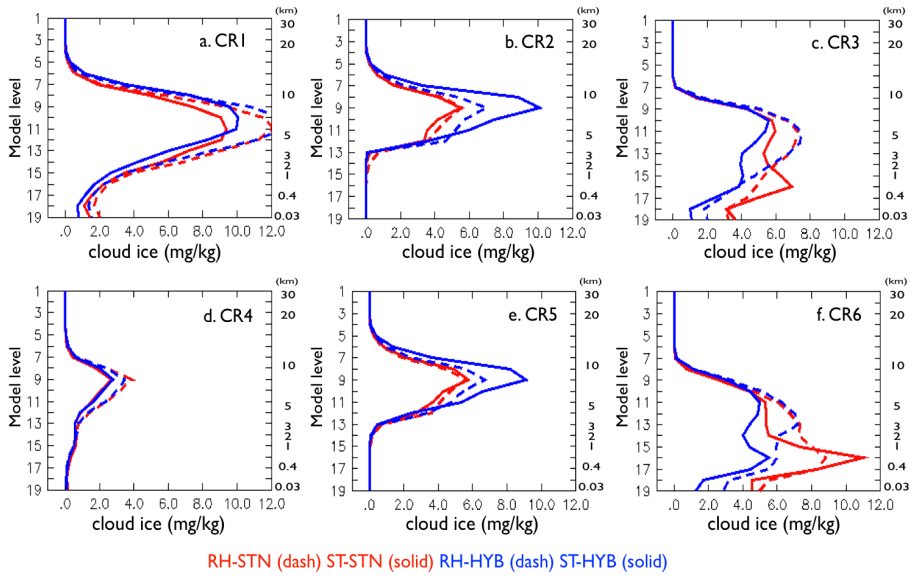


Fig. S7. Vertical distributions of cloud ice in the selected continental regions (CR) for RH-STN, ST-STN, RH-HYB, and ST-HYB.

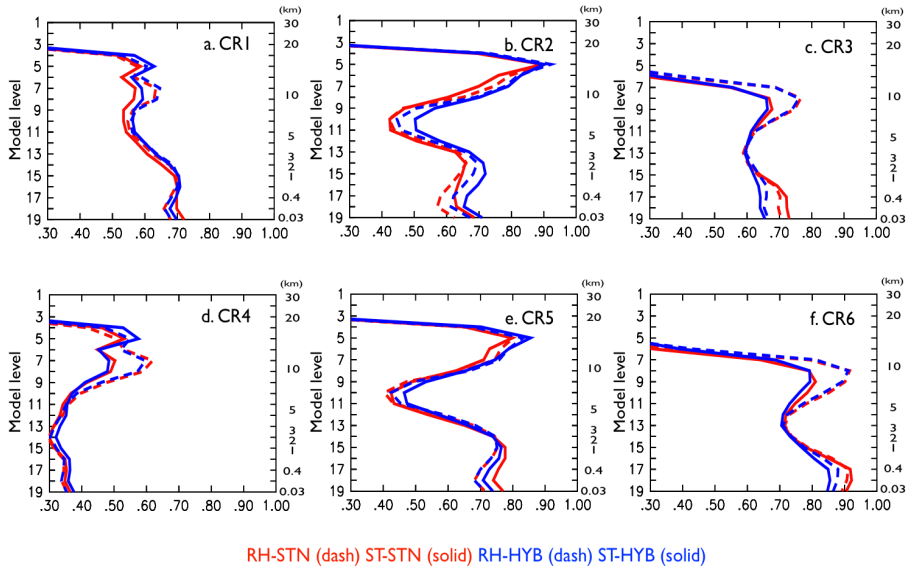


Fig. S8. Vertical distributions of relative humidity in the selected continental regions (CR) for RH-STN, ST-STN, RH-HYB, and ST-HYB.

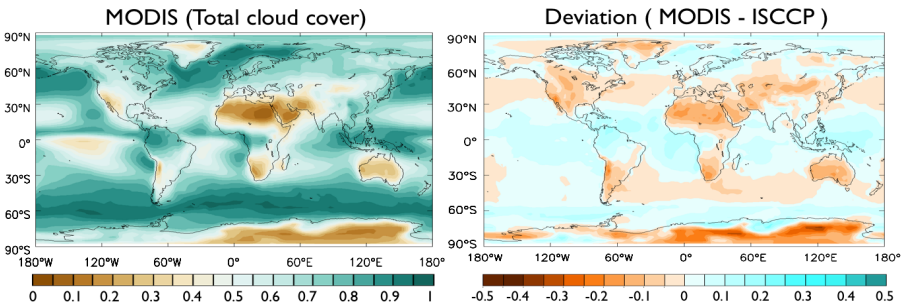


Fig. S9. Global distributions of total cloud cover fraction (TCC) derived by MODIS over a 10 year period and the difference of TCC between MODIS and ISCCP [MODIS-ISCCP].

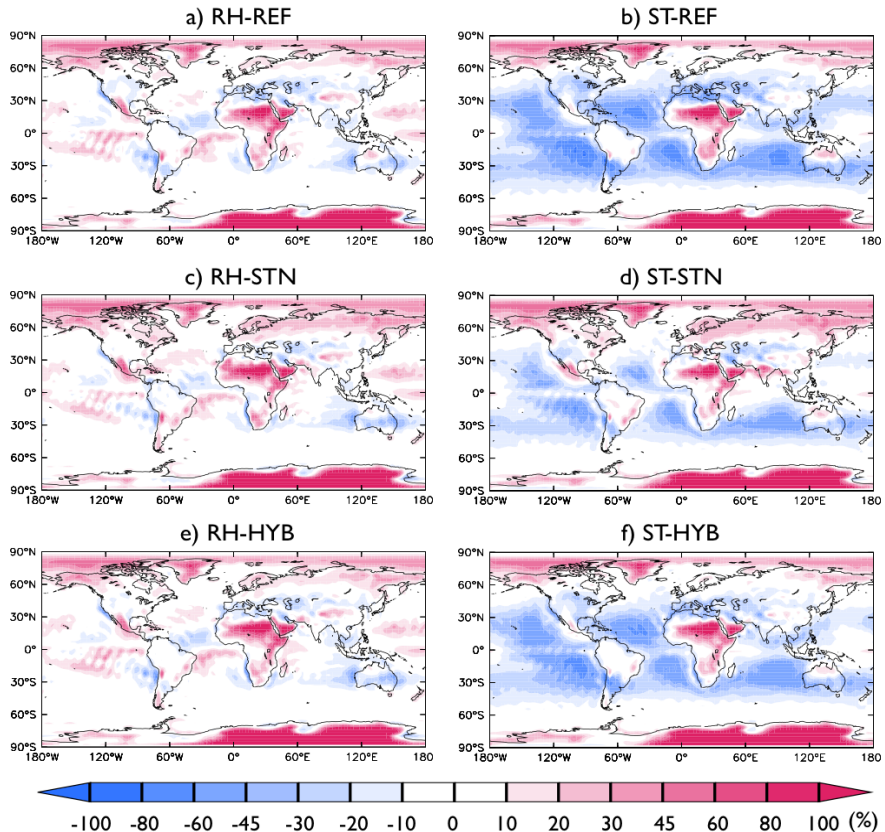


Fig. S10. Relative differences of TCC between simulations and observations (OBS) by MODIS over 10 years: Relative difference (%) = $\frac{[Model - OBS]}{OBS} \times 100\%$

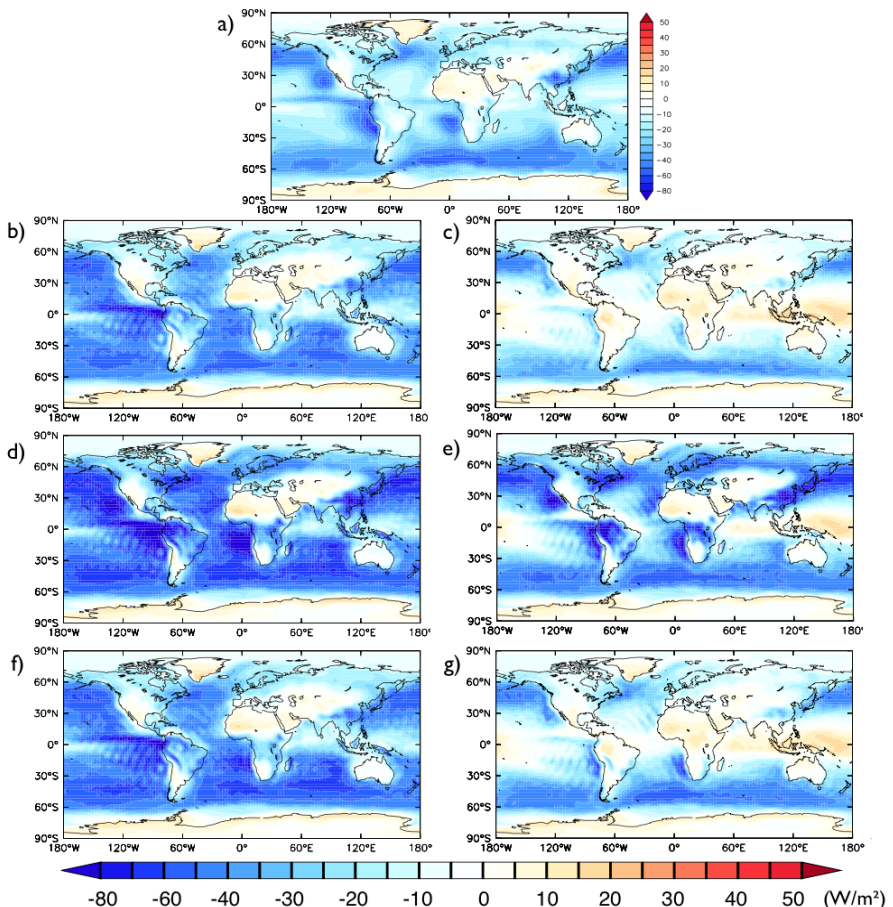


Fig. S11. Annual mean of NCRE at TOA for the simulations and the observational data: a) CERES EBAF (OBS), b) RH-REF, c) ST-REF, d) RH-STN, e) ST-STN, f) RH-HYB and g) ST-HYB

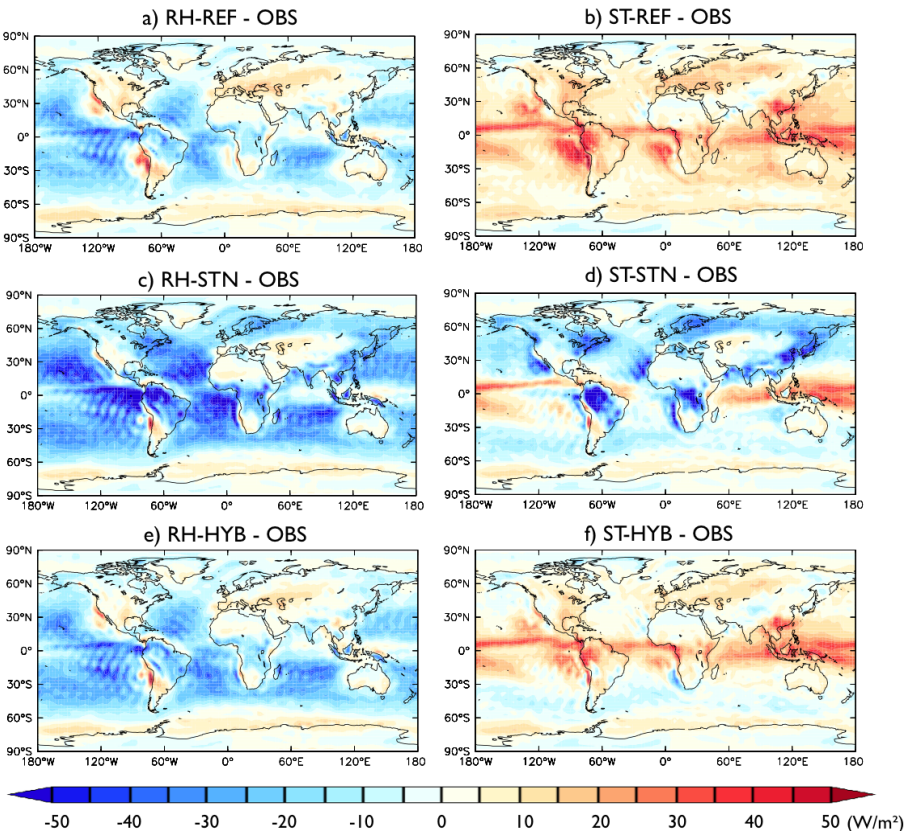


Fig. S12. Deviations of annual mean NCRE at TOA between the simulations and the observational data (CERES EBAF); a) RH-REF, b) ST-REF, c) RH-STN, d) ST-STN, e) RH-HYB, f) ST-HYB